Journal of Alloys and Compounds 695 (2017) 567–573

Contents lists available at ScienceDirect

Journal of Alloys and Compounds

journal homepage: http://www.elsevier.com/locate/jalcom

Photoluminescence and charge compensation effects in $Lu_3Mg_yAl_{5-x-y}Si_xO_{12}:Ce^{3+}$ phosphors for white LEDs

Jun Qiao [a, b], Leijun Shen [b, *], Wenge Xiao [c], Xin Qiao [b], Zhongzhi Wang [b], Lele Gao [b], Bo Li [b], Yongbo Zhou [b], Xia Zhang [c], Xiyan Zhang [a, **]

[a] School of Materials Science and Engineering, Changchun University of Science and Technology, Changchun 130022, China
[b] Baotou Research Institute of Rare Earths, Baotou 014030, China
[c] State Key Laboratory of Luminescence and Applications, Changchun Institute of Optics, Fine Mechanics and Physics, Chinese Academy of Sciences, Changchun 130033, China

ARTICLE INFO

Article history:
Received 22 July 2016
Received in revised form
6 November 2016
Accepted 8 November 2016
Available online 9 November 2016

Keywords:
Charge compensation effect
Photoluminescence
White LEDs
Phosphor

ABSTRACT

Phosphors with the nominal composition $Lu_{2.94}Ce_{0.06}Mg_yAl_{5-x-y}Si_xO_{12}$ ($x = 0–2$, $y = 0–2$) were synthesized by a conventional solid-state reaction in a reducing atmosphere (CO). The luminescence properties of these phosphors and the effect of charge compensation are discussed in detail. Our results indicate that the substitution of Mg^{2+} for Al^{3+} ions at octahedral coordination sites and the substitution of Si^{4+} for Al^{3+} ions at tetrahedral coordination sites are co-dependent processes because of charge compensation. Only when co-doping with Mg^{2+} and Si^{4+} ions, the incorporation of Mg^{2+} ions into octahedral coordination sites can be achieved. On incorporation of Mg^{2+} ions into the phosphor, an obvious red shift in the luminescence was observed. In addition, we analyzed the dependence of luminescence intensity on the absorptivity and the thermal quenching of the Ce^{3+} ions. The luminescence performances of white LEDs, fabricated by combining a single orange $Lu_{2.94}Ce_{0.06}Mg_2AlSi_2O_{12}$ phosphor with blue LED chips, were determined, which demonstrate the potential of this orange phosphor for use in warm white LEDs.

1. Introduction

Nowadays, phosphor-converted white light-emitting diodes (LEDs) are widely used in solid-state lighting and display areas because of their high luminous efficiency, low power consumption, reliability, long operation life, and environmental friendliness compared with conventional lighting sources like incandescent lamps and fluorescent lamps [1,2]. The most common phosphor-converted white LEDs are fabricated by combining blue InGaN LED chips with the yellow $Y_3Al_5O_{12}:Ce^{3+}$ ($YAG:Ce^{3+}$) phosphor [3,4]. However, these devices emit little red light and, therefore, have a poor color rendering index (CRI < 75) and high correlated color temperature (CCT ≈ 6000 K) [3,4]. To increase the red emission of these white LEDs, the blending of the yellow $YAG:Ce^{3+}$ phosphor and a red phosphor has been proposed, and some novel red phosphors based on Eu^{2+}-doped nitrides have been found [5–7]. However, these red phosphors require harsh preparation conditions like high temperatures, high pressures, and expensive raw materials. In addition, the blending of different phosphors generally results in poor chromatic stability of white LEDs. Until now, it has been believed that using a single-phase phosphor with sufficient red emission is the most reliable and economical way to achieve LEDs with a warm white color [8].

To achieve a high CRI and a low CCT in phosphor-converted white LEDs, various methods have been investigated to tune and improve the luminescence properties of current phosphors. These techniques include component substitution. For example, to enrich the red emissions of the $YAG:Ce^{3+}$ phosphor, the substitution of Gd^{3+} for Y^{3+} [9], Si^{4+}-N^{3-} for Al^{3+}-O^{2-} [10], and Mg^{2+}–Si^{4+}/Ge^{4+} for Al^{3+}–Al^{3+} [11,12] in the YAG host has been carried out. In addition, very recently, different component substitution strategies have been proposed and summarized, such as cation/anion substitution in $CaSrSi_{1-x}Al_xO_4:Ce^{3+}$, Li^+ [13], $Ca_{1.65}Sr_{0.35}Si_{1-x}(Al/Ga/B)_xO_4:Ce^{3+}$ [14], $Ca_2MgSi_2O_{7-x}N_x:Eu^{2+}$ [15], and $Lu_xSr_{2-x}SiN_xO_{4-x}:Eu^{2+}$ [16] and chemical unit co-substitution in $Ca_2(Al_{1-x}Mg_x)(Al_{1-x}Si_{1+x})$

* Corresponding author.
** Corresponding author.
E-mail addresses: wangshenleijun@126.com (L. Shen), xiyzhang@126.com (X. Zhang).

http://dx.doi.org/10.1016/j.jallcom.2016.11.094
0925-8388/

O_7:Eu^{2+} [17], $(CaMg)_x(NaSc)_{1-x}Si_2O_6$:$Eu^{2+}$ [18], and $(Ca_{1-x}Li_x)(Al_{1-x}Si_{1+x})N_3$:$Eu^{2+}$ [19].

$Lu_3Al_5O_{12}$:Ce^{3+} (LAG:Ce^{3+}) is a green phosphor with a high quantum efficiency and excellent thermal stability [20]. Recently, via the substitution of the Mg^{2+}-Si^{4+} pair for the Al^{3+}-Al^{3+} pair in the LAG host, a novel yellow $Lu_3MgAl_3SiO_{12}$:Ce^{3+} phosphor has been obtained [21]. In the structure of this phosphor, Mg^{2+} and Si^{4+} ions occupy the octahedral and tetrahedral coordination sites, respectively. In addition, the crystal structure evolution and tunable photoluminescence of $Lu_3(Al_{2-x}Mg_x)(Al_{3-x}Si_x)O_{12}$:$Ce^{3+}$ and $Lu_{3-x}Y_xMgAl_3SiO_{12}$:$Ce^{3+}$ phosphors have been reported [22,23]. Furthermore, a similar tunable photoluminescence has been achieved in a series of Ce^{3+}-activated $Lu_3Al_5O_{12}$–$Lu_2CaMg_2Si_3O_{12}$ solid-solution phosphors [24]. The luminescence red shift of the Mg-Si co-doped LAG:Ce^{3+} phosphors has been attributed to the lower transition energy of Ce^{3+} ions between the lowest 5d state and the 4f ground state, which is mainly caused by the presence of Mg^{2+} ions at the octahedral coordination sites [21–23]. However, the effects of charge compensation on the incorporation of Mg^{2+} ions into the octahedral coordination sites and the photoluminescence of phosphors have not been analyzed in detail.

We have studied the effect of charge compensation on the substitution of Mg^{2+} for Al^{3+} ions at octahedral coordination sites by analyzing the changes in the luminescence of Mg-Si co-doped LAG:Ce^{3+} phosphors. In addition, the dependence of the luminescence intensity on the absorptivity and thermal quenching behavior of Ce^{3+} ions was analyzed. Finally, white LEDs with different emission spectra were fabricated by combining a single orange $Lu_{2.94}Ce_{0.06}Mg_2AlSi_2O_{12}$ phosphor with blue LED chips, and their luminescence performances were characterized.

2. Experimental

2.1. Materials and synthesis

$Lu_{2.94}Ce_{0.06}Mg_yAl_{5-x-y}Si_xO_{12}$ (x = 0–2, y = 0–2) phosphors were synthesized by a conventional solid-state reaction. The constituent oxides Lu_2O_3, MgO, Al_2O_3, SiO_2, and CeO_2 were used as the precursor materials. Mixtures of these raw materials were sintered in a muffle furnace at 1500 °C for 5 h in a reducing atmosphere (CO), which was produced by the incomplete combustion of carbon.

2.2. Measurements and characterization

The photoluminescence (PL), photoluminescence excitation (PLE), and diffuse reflectance (DR) spectra were measured by using HITACHI F-7000 spectrometer. In the measurement of DR spectra, $BaSO_4$ was used as reference compound. Powder X-ray diffraction (XRD) data were collected using Cu-K_α radiation (λ = 1.54056 Å) on a Bruker D8 advance diffractometer. The Ce^{3+} fluorescence decay curves were measured by using a FL920 fluorescence lifetime spectrometer (Edinburgh Instruments Ltd.). The white LEDs were fabricated by coating the mixture of phosphor and epoxy resin on InGaN LED chips. The CRI, CCT, and chromaticity coordinates of the white LEDs were measured using an Ocean Optics USB4000 spectrometer.

3. Results and discussion

Fig. 1(a) shows the crystal structure of LAG, which crystallizes in the cubic space group $Ia\bar{3}d$. In the LAG structure, there are two different Al^{3+} sites: an octahedral coordination site and a tetrahedral coordination site [21,22], and these are denoted as Al^{3+}(I) and Al^{3+}(II), respectively; the occupation ratio at these sites is 2:3. For the Mg-Si co-doped LAG:Ce^{3+} phosphor, the structural refinement data indicate that Ce^{3+} and Lu^{3+} ions are randomly distributed over the dodecahedral coordination sites, Mg^{2+} and Al^{3+}(I) are randomly distributed over the octahedral coordination sites, and Si^{4+} and Al^{3+}(II) are randomly distributed over the tetrahedral coordination sites [21,22].

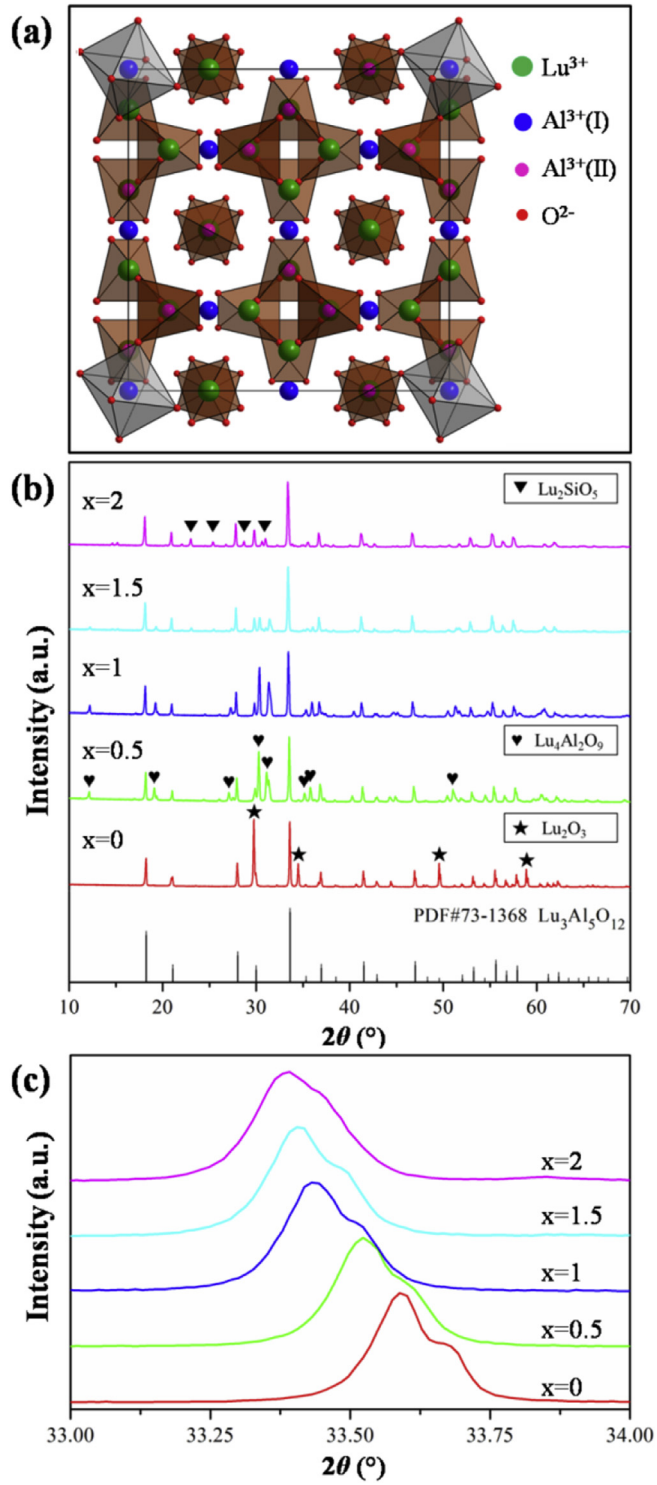

Fig. 1. (a) A schematic crystal structure of LAG viewed along the c-axis, (b) XRD patterns for $Lu_{2.94}Ce_{0.06}Mg_2Al_{3-x}Si_xO_{12}$ (x = 0–2) phosphors, and (c) XRD patterns for $Lu_{2.94}Ce_{0.06}Mg_2Al_{3-x}Si_xO_{12}$ (x = 0–2) phosphors in the 2θ range of 33–34°.

To study the effect of charge compensation in the Mg-Si co-doped LAG:Ce^{3+} phosphors, we synthesized a series of samples with the nominal composition of $Lu_{2.94}Ce_{0.06}Mg_2Al_{3-x}Si_xO_{12}$ ($x = 0–2$). Fig. 1(b) shows the XRD patterns of these samples. All the XRD patterns contain high-intensity peaks arising from the LAG garnet phase (JCPDF No. 73-1368); however, peaks arising from impurity phases are also visible. When $x = 0$, the sample has a nominal composition of $Lu_{2.94}Ce_{0.06}Mg_2Al_3O_{12}$, in which the substitution of Mg^{2+} for Al^{3+}(I) was attempted. Unfortunately, the luminescence characteristics of this sample (see below) indicate that, without the substitution of Si^{4+} for Al^{3+}(II), the substitution of Mg^{2+} for Al^{3+}(I) in this sample does not occur because of the charge mismatch between Mg^{2+} and Al^{3+}(I). Notably, in this sample, only one impurity phase is observed, Lu_2O_3 (JCPDF No. 86-2475), and, despite the large amount of MgO added during synthesis, no Mg^{2+}-containing phase is observed. A possible reason for the lack of a Mg^{2+}-containing phase is that unreacted MgO was reduced to Mg by the reducing atmosphere (CO); then, Mg, which has a higher vapor pressure than the other constituents, sublimed from the sample during synthesis. When $x = 0.5$ and 1, the decrease in the nominal Al^{3+} content promoted the formation of a $Lu_4Al_2O_9$ phase, and the diffraction peaks corresponding to this phase are present in the corresponding XRD patterns. When $x = 2$ (i.e., when the nominal content of Si^{4+} is equal to that of Mg^{2+}), the diffraction peaks arising from the $Lu_4Al_2O_9$ phase disappear, and some low-intensity peaks arising from a Lu_2SiO_5 phase (JCPDF No. 41-0239) appear. Possibly, the loss of Mg^{2+} by sublimation resulted in the extra Si^{4+} from the precursor materials not being incorporated into the Al^{3+}(II) sites. The substitution of Mg^{2+} for Al^{3+}(I) and the substitution of Si^{4+} for Al^{3+}(II) probably proceed simultaneously and promote each other due to charge compensation effects.

In the LAG structure, the radii of Al^{3+}(I) and Al^{3+}(II) ions are 0.67 and 0.53 Å, respectively, and the radii of Mg^{2+} ions at octahedral coordination sites and Si^{4+} ions at tetrahedral coordination sites are 0.86 and 0.40 Å, respectively [11,12,25]. The substitution of Si^{4+} for Al^{3+}(II) at the tetrahedral coordination sites not only compensates for the charge mismatch but also for the lattice expansion caused by the substitution of the larger Mg^{2+} ions for Al^{3+}(I) at the octahedral coordination sites. Comparing the difference between the ionic radius of Mg^{2+} and that of Al^{3+}(I) with the difference between the ionic radii of Si^{4+} and Al^{3+}(II), we infer that the substitution of the Mg^{2+}-Si^{4+} pair for the Al^{3+}(I)-Al^{3+}(II) pair in the LAG host results in lattice expansion; this was confirmed by the observation of a slight peak shift towards smaller 2θ angles of the LAG phase (see Fig. 1(c)). The lattice parameters for $Lu_{2.94}Ce_{0.06}Mg_2Al_{3-x}Si_xO_{12}$ ($x = 0–2$) were also calculated. As shown in Table 1, with increasing x, the unit cell becomes larger.

Notably, the impurity phases do not affect the study of the luminescence properties of the as-synthesized phosphors significantly because Lu_2O_3:Ce^{3+}, $Lu_4Al_2O_9$:Ce^{3+}, and Lu_2SiO_5:Ce^{3+} cannot be effectively excited by the blue light ($\lambda = 450$ nm) that was used for excitation in our experiments [26–28].

Fig. 2 shows the PLE and PL spectra for the $Lu_{2.94}Ce_{0.06}Mg_2Al_{3-x}Si_xO_{12}$ ($x = 0–2$) and LAG:Ce^{3+} phosphors. The LAG:Ce^{3+} phosphor exhibits an intense green emission band, which is attributed to the transitions from the lowest Ce^{3+} 5d excited state to the two 4f ground state levels ($^2F_{5/2}$ and $^2F_{7/2}$) [21–23]. The PLE spectrum of the Ce^{3+} ions in LAG contains two bands: a strong band around 450 nm and a relatively weak band around 350 nm, which are attributed to the transitions from the 4f ground state to the lowest and upper 5d excited-state levels ($^2D_{5/2}$, $^2D_{3/2}$), respectively [21–23]. The PLE band around 450 nm well matches the emission wavelength of blue InGaN LEDs. In the series of $Lu_{2.94}Ce_{0.06}Mg_2Al_{3-x}Si_xO_{12}$ ($x = 0–2$) phosphors, the sample with $x = 0$ exhibits similar PL and PLE bands to those of the LAG:Ce^{3+} phosphor. However, with increasing x, the PL band and the PLE band around 450 nm shift towards longer wavelengths. Meanwhile, a clear change in the PLE band around 350 nm was observed, which is mainly ascribed to the absorptions of impurity phosphors like Lu_2O_3:Ce^{3+}, $Lu_4Al_2O_9$:Ce^{3+}, and Lu_2SiO_5:Ce^{3+}.

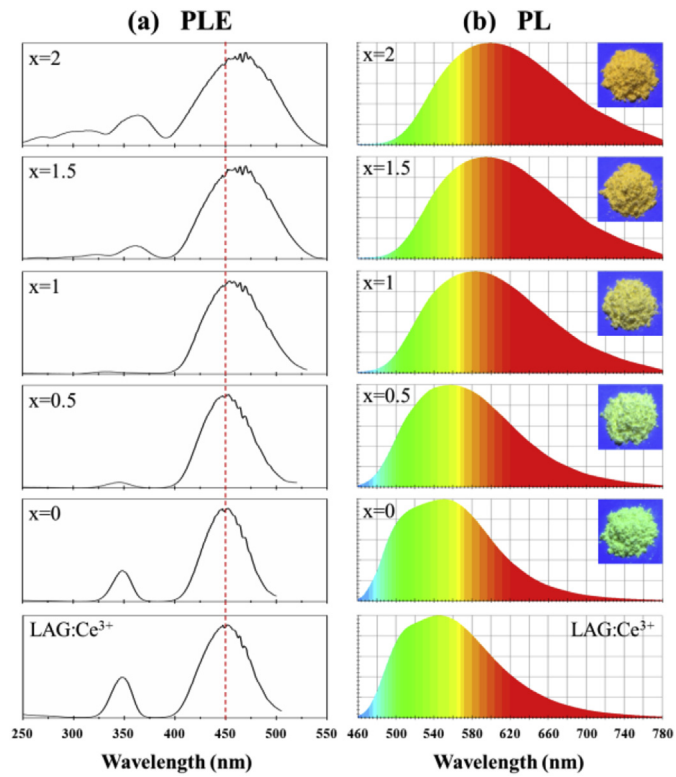

Fig. 2. (a) PLE spectra and (b) PL spectra for $Lu_{2.94}Ce_{0.06}Mg_2Al_{3-x}Si_xO_{12}$ ($x = 0–2$) and LAG:Ce^{3+} phosphors. The insets photographs show the phosphors under blue light excitation. (For interpretation of the references to colour in this figure legend, the reader is referred to the web version of this article.)

The red-shift $D(A)$ of the 4f-5d transition of Ce^{3+} in the phosphor relative to the free-ion value can be written as

$$D(A) = \varepsilon_c(A) + \frac{\varepsilon_{cfs}(A)}{r(A)} - 1890\text{cm}^{-1}$$

$D(A)$ is dependent upon two factors, the centroid shift $\varepsilon_c(A)$, which is defined as the lowering of the average energy of the Ce^{3+} 5d configuration relative to the value for Ce^{3+} as a free ion, and the crystal field splitting $\varepsilon_{cfs}(A)$, which is defined as the energy difference between the lowest and the highest 5d-level. $r(A)$ is a constant in certain coordination environments [25,29]. The centroid shift, $\varepsilon_c(A)$, is affected by the covalent character of the host lattice. In studies of $Y_3Mg_2AlSi_2O_{12}$:Ce^{3+} and $Tb_3Mg_xAl_{5-2x}Si_xO_{12}$:$Ce^{3+}$ phosphors, the increased covalent character of the host lattice due

Table 1
Lattice parameters for $Lu_{2.94}Ce_{0.06}Mg_2Al_{3-x}Si_xO_{12}$ ($x = 0–2$) phosphors.

Composition (x)	Lattice parameter (Å)
0	11.9216
0.5	11.9447
1	11.9701
1.5	11.9776
2	11.9855

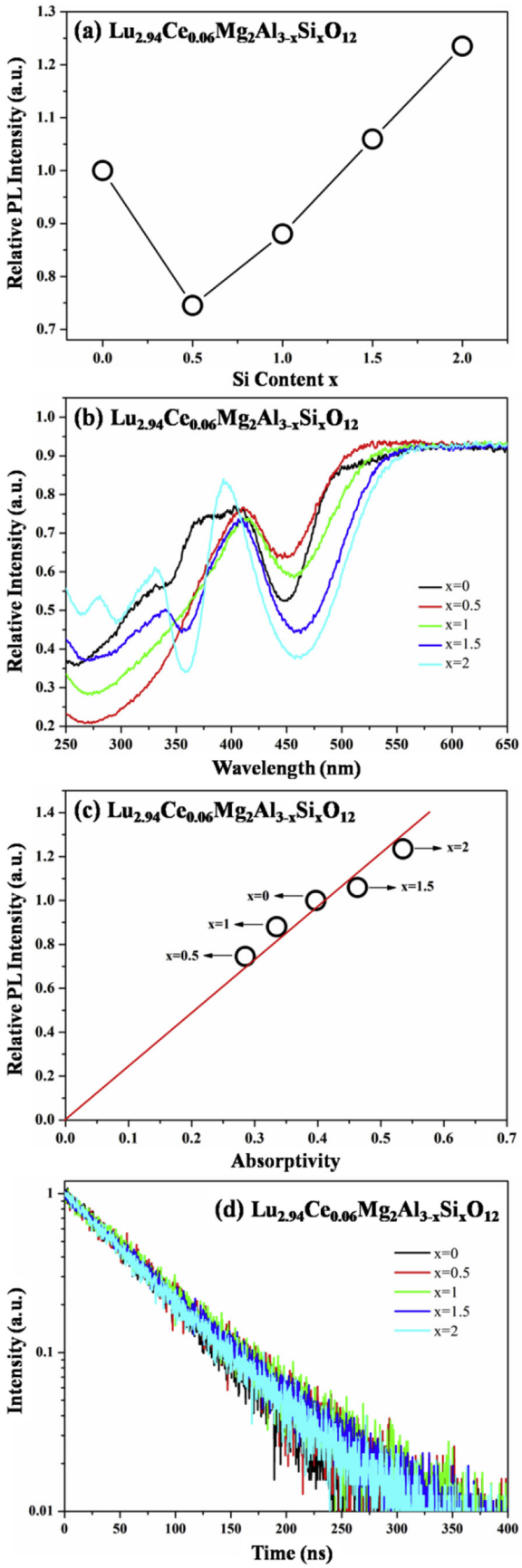

Fig. 3. (a) The change of relative PL intensities of $Lu_{2.94}Ce_{0.06}Mg_2Al_{3-x}Si_xO_{12}$ ($x = 0–2$) phosphors as a function of x, (b) DR spectra for $Lu_{2.94}Ce_{0.06}Mg_2Al_{3-x}Si_xO_{12}$ ($x = 0–2$) phosphors, (c) the change of relative PL intensities of $Lu_{2.94}Ce_{0.06}Mg_2Al_{3-x}Si_xO_{12}$ ($x = 0–2$) phosphors as a function of absorptivity around 450 nm, and (d) fluorescence decay curves of Ce^{3+} ions (excited at 450 nm and monitored at 550 nm) in $Lu_{2.94}Ce_{0.06}Mg_2Al_{3-x}Si_xO_{12}$ ($x = 0–2$) phosphors.

to the presence of Mg^{2+} ions at Al^{3+}(I) sites has been considered a possible reason for the red shift in the luminescence [11,25]. In our case, a similar reason can also be used to interpret the red shift in the luminescence. The crystal field splitting, $\varepsilon_{cfs}(A)$, is proportional to R^{-5}, where R is the Ce^{3+}–O^{2-} distance [25]. From the viewpoint of the crystal structure [22,23], the substitution of larger radius Mg^{2+} ions for smaller radius Al^{3+}(I) ions in the garnet structure results in the compression of the polyhedrons around Ce^{3+}. The decrease in R may lead to a larger crystal field splitting, as in the case reported by J. Ueda et al. [30,31].

Based on the above analysis, we believe that the value of the spectral red shift is closely related to the number of Mg^{2+} ions incorporated into Al^{3+}(I) sites. In the sample with $x = 0$, Mg^{2+} ions from precursor materials were not incorporated into the Al^{3+}(I) sites due to the charge mismatch between Mg^{2+} and Al^{3+}(I) ions. However, by increasing x, the number of Mg^{2+} ions incorporated into Al^{3+}(I) sites can be increased markedly by the doping of Si^{4+} ions into the Al^{3+}(II) sites, which is induced by charge compensation effects. Finally, via the charge balancing substitution of the Mg^{2+}-Si^{4+} pair for the Al^{3+}-Al^{3+} pair, the green LAG:Ce^{3+} phosphor gradually became an orange phosphor. A similar charge compensation effect has been discussed in Al^{3+}-doped Sr_2SiO_4:Eu^{2+}/Eu^{3+} phosphors, where the incorporation of Al^{3+} ions into Si^{4+} sites caused the stabilization of the Eu^{3+} ions at Sr^{2+} sites under a reducing atmosphere due to the charge compensation effect [32].

In addition, with respect to Fig. 2, the broadening of the PL band with increasing x can be attributed to the inhomogeneous broadening of the Ce^{3+} ion luminescence, which is caused by the greater diversity of local environments of Ce^{3+} ions in the Mg-Si co-doped LAG host [22,25]. The broader emission band is beneficial to the achievement of greater color rendering in white LEDs.

Fig. 3(a) shows the change in the relative PL intensity of the $Lu_{2.94}Ce_{0.06}Mg_2Al_{3-x}Si_xO_{12}$ ($x = 0–2$) phosphors as a function of x, where the integrated PL intensity of $Lu_{2.94}Ce_{0.06}Mg_2Al_3O_{12}$ is set as the normalized standard. The DR spectra of these samples were also measured, as shown in Fig. 3(b). The absorption band around 450 nm is attributed to the transition from the Ce^{3+} 4f ground state to the Ce^{3+} 5d excited state. The slight red shift with increasing x agrees well with the changes in the PLE spectra of these samples. The absorptivity of Ce^{3+} around 450 nm in the samples can be easily obtained from the DR spectra. The dependence of the integrated PL intensity on the absorptivity of Ce^{3+} around 450 nm is plotted in Fig. 3(c), and the relative PL intensity is proportional to the absorptivity of Ce^{3+} around 450 nm. The linear relationship between the PL intensity and the absorptivity of Ce^{3+} indicates that the internal quantum efficiency of these phosphors changes little with the addition of Si^{4+}. To confirm this, we measured the fluorescence decay curves of Ce^{3+} ions in the phosphors. Fig. 3(d) shows the decay curves that can be well fitted with a single exponential function of $I(t)/I(0) = \exp(-t/\tau)$, where $I(t)$ is the luminescence intensity at time t, and τ is the lifetime. In the $Lu_{2.94}Ce_{0.06}Mg_2Al_{3-x}Si_xO_{12}$ ($x = 0–2$) phosphors, the decay curves do not change with increasing x, and the fluorescence lifetimes of the Ce^{3+} ions in these samples were all estimated to be about 66 ns. This result confirms that the internal quantum efficiency of these phosphors is almost unchanged on the introduction of Si^{4+} ions. Accordingly, the enhanced PL intensity is mainly attributed to the

Table 2
The chromaticity coordinates (x, y) for $Lu_{2.94}Ce_{0.06}Mg_2Al_{3-x}Si_xO_{12}$ ($x = 0–2$) phosphors.

Composition (x)	(x, y)
0	(0.376, 0.551)
0.5	(0.425, 0.533)
1	(0.483, 0.499)
1.5	(0.510, 0.480)
2	(0.520, 0.472)

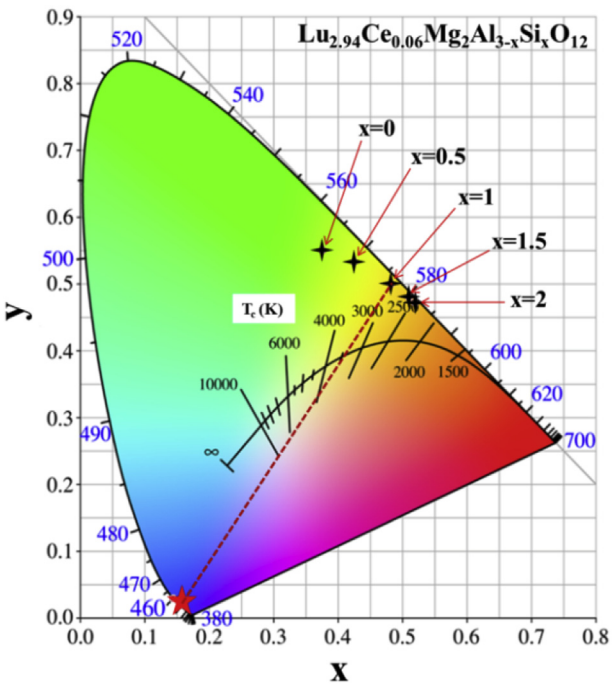

Fig. 4. The CIE 1931 chromaticity diagram with points indicating chromaticity coordinates for $Lu_{2.94}Ce_{0.06}Mg_2Al_{3-x}Si_xO_{12}$ ($x = 0–2$) phosphors.

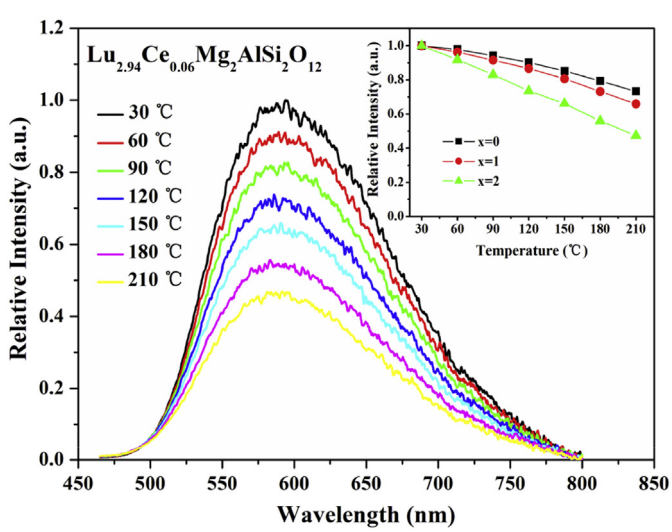

Fig. 5. The PL spectra for $Lu_{2.94}Ce_{0.06}Mg_2Al_{3-x}Si_xO_{12}$ ($x = 2$) phosphors at different temperatures. The inset is the changes of relative PL intensities of $Lu_{2.94}Ce_{0.06}Mg_2Al_{3-x}Si_xO_{12}$ ($x = 0, 1, 2$) phosphors as a function of temperature.

increase of the absorptivity of the Ce^{3+} ions.

The calculated chromaticity coordinates for the $Lu_{2.94}Ce_{0.06}Mg_2Al_{3-x}Si_xO_{12}$ ($x = 0–2$) phosphors are listed in Table 2, and the corresponding positions in the chromaticity diagram are shown as crosses in Fig. 4. On increasing x from 0 to 2, the chromaticity coordinates (x, y) change from (0.376, 0.551) to (0.520, 0.472), as shown in Table 2. Meanwhile, the emission color changes from green to orange under blue light excitation. The line connecting the chromaticity point of the blue LED with that of the phosphor crosses the blackbody locus at one point, and the CCT of this point can be obtained by combining the blue LED with the corresponding phosphor. Using Fig. 4, we found that warm white light with a CCT below 4000 K can be achieved by combining blue LED chips with $Lu_{2.94}Ce_{0.06}Mg_2Al_{3-x}Si_xO_{12}$ ($x \geq 1$) phosphors. Therefore, the as-synthesized samples are potential yellow-orange phosphors for use in warm white LEDs.

The temperature dependences of the PL spectra for the $Lu_{2.94}Ce_{0.06}Mg_2Al_{3-x}Si_xO_{12}$ ($x = 0, 1, 2$) phosphors were measured, and the PL spectra for the $Lu_{2.94}Ce_{0.06}Mg_2AlSi_2O_{12}$ phosphor at

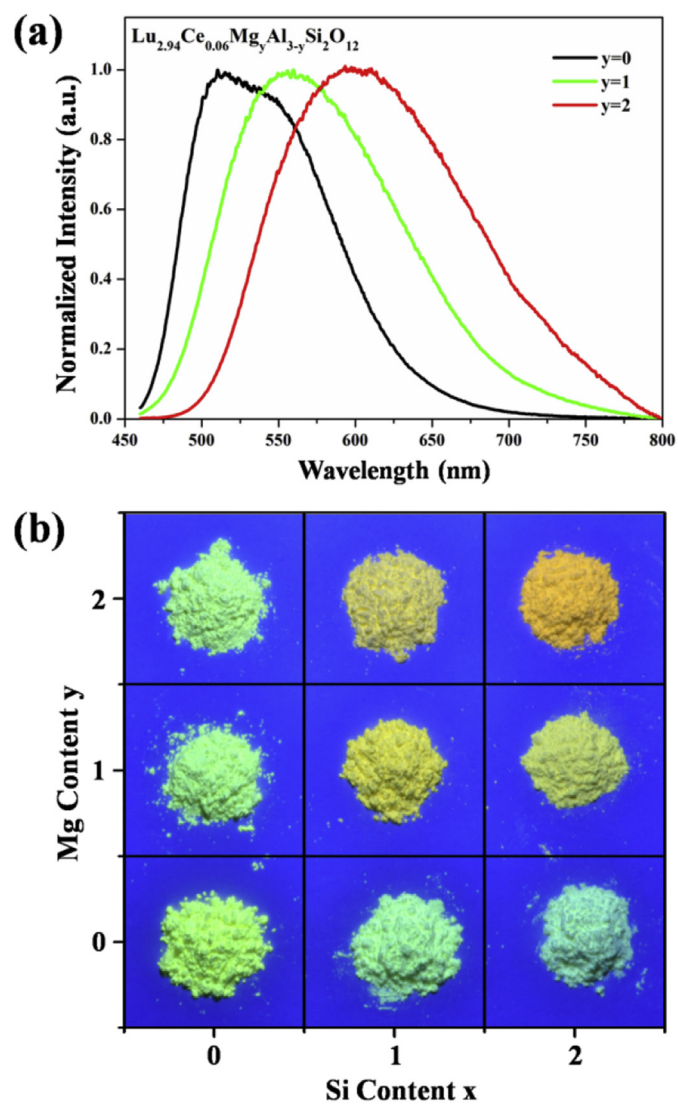

Fig. 6. (a) PL spectra for $Lu_{2.94}Ce_{0.06}Mg_yAl_{3-y}Si_2O_{12}$ ($y = 0–2$) phosphors and (b) photographs of $Lu_{2.94}Ce_{0.06}Mg_yAl_{5-x-y}Si_xO_{12}$ ($x = 0–2$, $y = 0–2$) phosphors under blue light excitation. (For interpretation of the references to colour in this figure legend, the reader is referred to the web version of this article.)

different temperatures are shown in Fig. 5 as representative spectra. The inset of Fig. 5 shows the changes in the relative PL intensities of the $Lu_{2.94}Ce_{0.06}Mg_2Al_{3-x}Si_xO_{12}$ ($x = 0, 1, 2$) phosphors as a function of temperature, where the integrated PL intensities at 30 °C are set as the normalized standard. On increasing the temperature, the PL intensities of these samples gradually decreased. In addition, the thermal quenching of the $Lu_{2.94}Ce_{0.06}Mg_2Al_{3-x}Si_xO_{12}$ ($x = 0, 1, 2$) phosphors increased as x increased. Using $I(T) = I(0)/(1 + A(\exp(\Delta E/k_BT)))$ with a constant A and the Boltzmann constant k_B, the activation energies (ΔE) of these samples were estimated to be 0.2527, 0.2441, and 0.2282 eV for $x = 0, 1, 2$, respectively. The increase of the thermal quenching with increasing x is probably attributed to the decrease of ΔE.

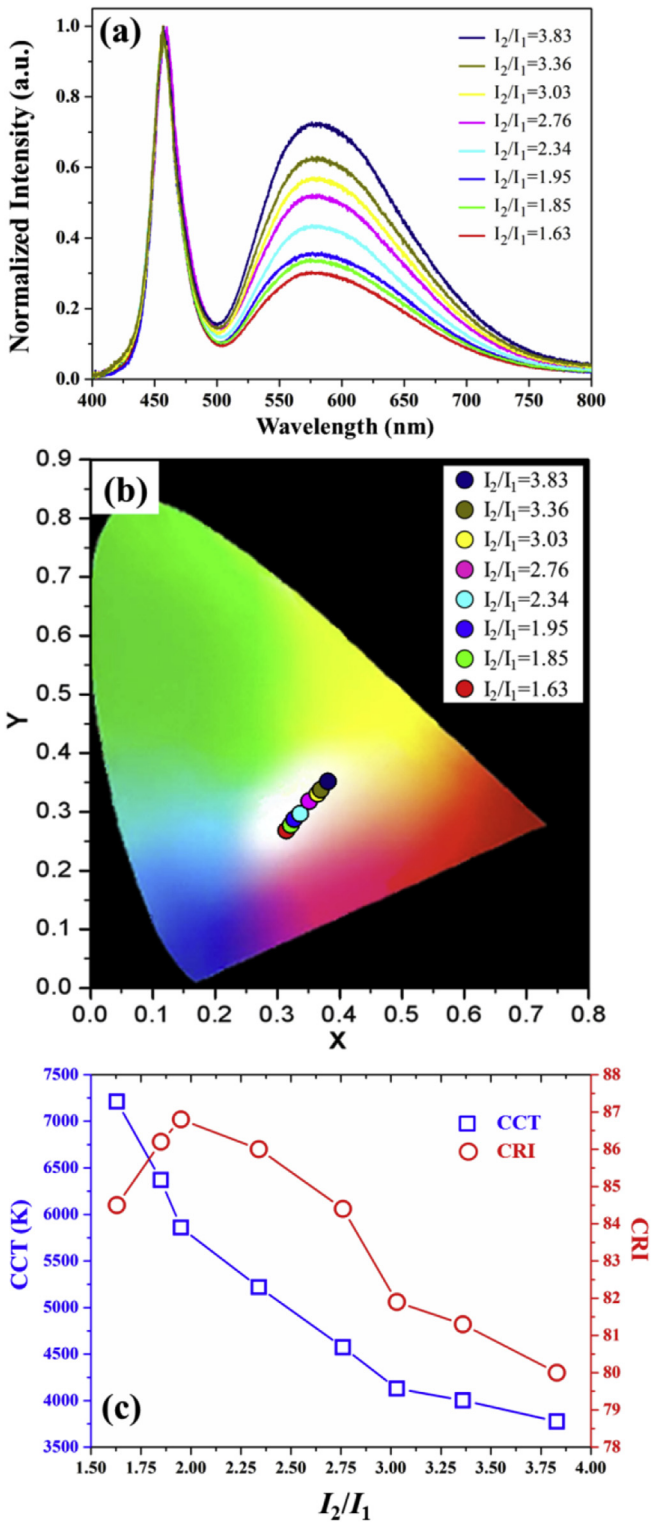

Fig. 7. (a) Emission spectra for the white LEDs fabricated by using a single $Lu_{2.94}Ce_{0.06}Mg_2AlSi_2O_{12}$ phosphor and InGaN LED (460 nm) chips, (b) the CIE 1931 chromaticity diagram with dots indicating chromaticity coordinates of the white LEDs with different values of I_2/I_1, and (c) the changes of CCT and CRI as a function of I_2/I_1.

To verify the charge compensation effects in the Mg-Si co-doped LAG:Ce^{3+} phosphors, we also synthesized $Lu_{2.94}Ce_{0.06}Mg_yAl_{5-x-y}Si_xO_{12}$ ($x = 0–2$, $y = 0–2$) phosphors with different Si^{4+} and Mg^{2+} contents. Fig. 6(a) shows the PL spectra for the $Lu_{2.94}Ce_{0.06}Mg_yAl_{3-y}Si_2O_{12}$ ($y = 0–2$) phosphors. When the Si^{4+} content was fixed at $x = 2$ and the Mg^{2+} content, y, was increased, similar spectral red shifts to those observed for $Lu_{2.94}Ce_{0.06}Mg_2Al_{3-x}Si_xO_{12}$ ($x = 0–2$) phosphors were observed. The red shifting is indicative of the increasing number of Mg^{2+} ions incorporated into Al^{3+}(I) sites. Fig. 6(b) shows photographs of the $Lu_{2.94}Ce_{0.06}Mg_yAl_{5-x-y}Si_xO_{12}$ ($x = 0–2$, $y = 0–2$) phosphors under blue light excitation. The emission color changes little in both the Si^{4+} singly doped samples and the Mg^{2+} singly doped samples; however, the emission color changes significantly in the Mg^{2+} and Si^{4+} co-doped samples. These results further demonstrate that the substitutions of Mg^{2+} for Al^{3+}(I) and Si^{4+} for Al^{3+}(II) are inseparable because charge compensation is necessary.

White LEDs can be fabricated by coating a mixture of a $Lu_{2.94}Ce_{0.06}Mg_2AlSi_2O_{12}$ phosphor and epoxy resin on InGaN LED (460 nm) chips. In our experiments, a series of white LEDs with different emission spectra were obtained by changing the coating amount, and their normalized emission spectra are shown in Fig. 7(a). We define the integrated luminescence intensities of blue LED chip and phosphor as I_1 and I_2, respectively. The luminescence properties of white LEDs depend largely on the ratio of I_2 to I_1. Fig. 7(b) shows the CIE 1931 chromaticity diagram, in which different color dots indicate chromaticity coordinates for the white LEDs with different values of I_2/I_1. The chromaticity coordinates (x, y) change from (0.314, 0.268) for the white LED with $I_2/I_1 = 1.63$ to (0.381, 0.352) for the white LED with $I_2/I_1 = 3.83$ in the white light area. The changes of CCT and CRI as a function of I_2/I_1 are shown in Fig. 7(c). As I_2/I_1 increases, the CCT monotonically decreases from 7211 to 3775 K, while the corresponding CRI increases first, reaching a maximum of 86.8 at $I_2/I_1 = 1.95$, and then decreases. Warm white LEDs with CCT <4200 K and CRI >80 were achieved when $I_2/I_1 > 3.03$, and the light generated by these LEDs is more favorable for general illumination compared to that produced by the white LEDs fabricated by combining the single YAG:Ce^{3+} phosphor with blue LED chips.

4. Conclusions

In summary, we have studied the effects of charge compensation on the substitution of Mg^{2+} ions for Al^{3+}(I) ions at octahedral coordination sites by analyzing the changes in the photoluminescence of $Lu_{2.94}Ce_{0.06}Mg_yAl_{5-x-y}Si_xO_{12}$ ($x = 0–2$, $y = 0–2$) phosphors. The results indicate that the substitution of Mg^{2+} for Al^{3+}(I) ions cannot be achieved without the substitution of Si^{4+} for Al^{3+}(II) ions because the charge difference between Mg^{2+} and Al^{3+}(I) ions must be compensated. The number of Mg^{2+} substituting for Al^{3+}(I) ions can be increased by substituting Si^{4+} for Al^{3+}(II) ions. Consequently, a phosphor with tunable photoluminescence, ranging in color from green to orange, was achieved. For the $Lu_{2.94}Ce_{0.06}Mg_2Al_{3-x}Si_xO_{12}$ ($x = 0–2$) phosphors, the linear relationship between the luminescence intensity and the absorptivity of Ce^{3+} ions suggests that the change of the luminescence

intensity is mainly attributed to the change of the absorptivity of Ce^{3+} ions rather than the internal quantum efficiency; this was also confirmed by the fluorescence decay curve measurements. The thermal quenching of the phosphors became stronger as the Si^{4+} content increased due to the decrease in the activation energy. Finally, we have also studied the luminescence properties of white LEDs fabricated by combining a single orange $Lu_{2.94}Ce_{0.06}Mg_2AlSi_2O_{12}$ phosphor with blue InGaN LED chips, and white LEDs with CRI >80 and CCT <4200 K were obtained.

Acknowledgements

This work was supported by the Natural Science Foundation of Inner Mongolia Autonomous Region (2016BS0101, 2016MS0524) and Postdoctoral Research Program of China Northern Rare Earth (group) High-Tech Co., Ltd. (2015H1894).

References

[1] N.C. George, K.A. Denault, R. Seshadri, Phosphors for solid-state white lighting, Annu. Rev. Mater. Res. 43 (2013) 481–501.
[2] Y.C. Lin, M. Karlsson, M. Bettinelli, Inorganic phosphor materials for lighting, Top. Curr. Chem. 374 (2016) 1–47.
[3] X.F. Li, J.D. Budai, F. Liu, J.Y. Howe, J.H. Zhang, X.J. Wang, Z.J. Gu, C.J. Sun, R.S. Meltzer, Z.W. Pan, New yellow Ba0. 93Eu0. 07Al2O4 phosphor for warm-white light-emitting diodes through single-emitting-center conversion, Light Sci. Appl. 2 (2013) e50.
[4] G.G. Li, Y. Tian, Y. Zhao, J. Lin, Recent progress in luminescence tuning of Ce^{3+} and Eu^{2+}-activated phosphors for pc-WLEDs, Chem. Soc. Rev. 44 (2015) 8688–8713.
[5] R.J. Xie, N. Hirosaki, T. Suehiro, F.F. Xu, M. Mitomo, A simple, efficient synthetic route to $Sr_2Si_5N_8$:Eu^{2+}-based red phosphors for white light-emitting diodes, Chem. Mater. 18 (2006) 5578–5583.
[6] J.W. Li, T. Watanabe, N. Sakamoto, H. Wada, T. Setoyama, M. Yoshimura, Synthesis of a multinary nitride, Eu-doped $CaAlSiN_3$, from alloy at low temperatures, Chem. Mater. 20 (2008) 2095–2105.
[7] P. Pust, V. Weiler, C. Hecht, A. Tücks, A.S. Wochnik, A.K. Henß, D. Wiechert, C. Scheu, P.J. Schmidt, W. Schnick, Narrow-band red-emitting Sr[$LiAl_3N_4$]:Eu^{2+} as a next-generation LED-phosphor material, Nat. Mater. 13 (2014) 891–896.
[8] M.M. Shang, C.X. Li, J. Lin, How to produce white light in a single-phase host? Chem. Soc. Rev. 43 (2014) 1372–1386.
[9] L. Kong, S.C. Gan, G.Y. Hong, J.L. Zhang, Relationship between crystal structure and luminescence properties of $(Y_{0.96-x}Ln_xCe_{0.04})_3Al_5O_{12}$ (Ln= Gd, La, and Lu), J. Rare Earths 25 (2007) 692–696.
[10] A.A. Setlur, W.J. Heward, M.E. Hannah, U. Happek, Incorporation of Si^{4+}–N^{3-} into Ce^{3+}-doped garnets for warm white LED phosphors, Chem. Mater. 20 (2008) 6277–6283.
[11] A. Katelnikovas, T. Bareika, P. Vitta, T. Jüstel, H. Winkler, A. Kareiva, A. Zukauskas, G. Tamulaitis, $Y_{3-x}Mg_2AlSi_2O_{12}$:xCe^{3+} phosphors-prospective for warm-white light emitting diodes, Opt. Mater. 32 (2010) 1261–1265.
[12] M.M. Shang, J. Fan, H.Z. Lian, Y. Zhang, D.L. Geng, J. Lin, A double substitution of Mg^{2+}–Si^{4+}/Ge^{4+} for $Al^{3+}_{(1)}$–$Al^{3+}_{(2)}$ in Ce^{3+}-doped garnet phosphor for white LEDs, Inorg. Chem. 53 (2014) 7748–7755.
[13] S.H. Miao, Z.G. Xia, M.S. Molokeev, M.Y. Chen, J. Zhang, Q.L. Liu, Effect of Al/Si substitution on the structure and luminescence properties of $CaSrSiO_4$:Ce^{3+} phosphors: analysis based on the polyhedral distortion, J. Mater. Chem. C 3 (2015) 4616–4622.
[14] K. Li, M.M. Shang, H.Z. Lian, J. Lin, Photoluminescence properties of efficient blue-emitting phosphor α-$Ca_{1.65}Sr_{0.35}SiO_4$:Ce^{3+}: color tuning via the substitutions of Si by Al/Ga/B, Inorg. Chem. 54 (2015) 7992–8002.
[15] Z. He, X.F. Huang, R.D. Zhou, W.G. Huang, Synthesis and luminescence properties of a new green emitting $Ca_2MgSi_2O_{7-x}N_x$:Eu^{2+} phosphor, J. Alloys Compd. 658 (2016) 36–40.
[16] Z.G. Xia, S.H. Miao, M.S. Molokeev, M.Y. Chen, Q.L. Liu, Structure and luminescence properties of Eu^{2+} doped $Lu_xSr_{2-x}SiN_xO_{4-x}$ phosphors evolved from chemical unit cosubstitution, J. Mater. Chem. C 4 (2016) 1336–1344.
[17] Z.G. Xia, C.G. Ma, M.S. Molokeev, Q.L. Liu, K. Rickert, K.R. Poeppelmeier, Chemical unit cosubstitution and tuning of photoluminescence in the $Ca_2(Al_{1-x}Mg_x)(Al_{1-x}Si_{1+x})O_7$:$Eu^{2+}$ phosphor, J. Am. Chem. Soc. 137 (2015) 12494–12497.
[18] Z.G. Xia, G.K. Liu, J.G. Wen, Z.G. Mei, M. Balasubramanian, M.S. Molokeev, L.C. Peng, L. Gu, D.J. Miller, Q.L. Liu, K.R. Poeppelmeier, Tuning of photoluminescence by cation nanosegregation in the $(CaMg)_x(NaSc)_{1-x}Si_2O_6$ solid solution, J. Am. Chem. Soc. 138 (2016) 1158–1161.
[19] T. Wang, Q.C. Xiang, Z.G. Xia, J. Chen, Q.L. Liu, Evolution of structure and photoluminescence by cation cosubstitution in Eu^{2+}-doped $(Ca_{1-x}Li_x)(Al_{1-x}Si_{1+x})N_3$ solid solutions, Inorg. Chem. 55 (2016) 2929–2933.
[20] K. Parka, T. Kimb, Y. Yub, K. Seoc, J. Kima, Y/Gd-free yellow $Lu_3Al_5O_{12}$:Ce^{3+} phosphor for white LEDs, J. Lumin 173 (2016) 159–164.
[21] Y.R. Shi, G. Zhu, M. Mikami, Y. Shimomura, Y.H. Wang, A novel Ce^{3+} activated $Lu_3MgAl_3SiO_{12}$ garnet phosphor for blue chip light-emitting diodes with excellent performance, Dalton Trans. 44 (2015) 1775–1781.
[22] H.P. Ji, L. Wang, M.S. Molokeev, N. Hirosaki, R.J. Xie, Z.H. Huang, Z.G. Xia, O.M. ten Kate, L.H. Liu, V.V. Atuchin, Structure evolution and photoluminescence of $Lu_3(Al,Mg)_2(Al,Si)_3O_{12}$:$Ce^{3+}$ phosphors: new yellow-color converters for blue LED-driven solid state lighting, J. Mater. Chem. C 4 (2016) 6855–6863.
[23] H.P. Ji, L. Wang, M.S. Molokeev, N. Hirosaki, Z.H. Huang, Z.G. Xia, O.M. ten Kate, L.H. Liu, R.J. Xie, New garnet structure phosphors, $Lu_{3-x}Y_xMgAl_3SiO_{12}$:$Ce^{3+}$ (x=0–3), developed by solid solution design, J. Mater. Chem. C 4 (2016) 2359–2366.
[24] Y.B. Chen, Z.B. Tang, X.S. Xu, D.H. Feng, Z.Z. Wang, Z.Q. Liu, Tunable photoluminescence in $Lu_3Al_5O_{12}$–$Lu_2CaMg_2Si_3O_{12}$ solid solution phosphors manipulated by synchronous ions co-substitution, RSC Adv. 6 (2016) 43916–43923.
[25] H.D. Luo, J. Liu, X. Zheng, B. Xu, Y.M. Lu, L.X. Han, K.X. Ren, X.B. Yu, Synthesis and luminescence properties of Mg–Si co-doped $Tb_3Al_5O_{12}$:Ce^{3+} phosphors with blue excitation for white LEDs, J. Am. Ceram. Soc. 95 (2012) 3582–3587.
[26] M. Raukas, S. Basun, W.M. Dennis, D.R. Evans, U. Happek, W.V. Schaik, W.M. Yen, Optical properties of Ce^{3+} doped Lu_2O_3 and Y_2O_3 single crystals, J. SID 4 (1996) 189–192.
[27] Y.Z. Wang, Q.Y. He, B.L. Chu, Synthesis and characterization of Ce-doped Lu_2SiO_5 powders by the solid-state reaction with Li_2SO_4 flux, J. Alloys Compd. 479 (2009) 704–706.
[28] L. Zhang, C. Madej, C. Pedrini, B. Moine, C. Dujardin, A. Petrosyan, A.N. Belsky, Elaboration and spectroscopic properties of new dense cerium-doped lutetium based scintillator materials, Chem. Phys. Lett. 268 (1997) 408–412.
[29] P. Dorenbos, Optical basicity, interpreted by means of Ce^{3+} 5d level spectroscopy in ionic crystals, J. Non Cryst. Solids 324 (2003) 220–229.
[30] S. Mahlik, A. Lazarowska, J. Ueda, S. Tanabe, M. Grinberg, Spectroscopic properties and location of the Ce^{3+} energy levels in $Y_3Al_2Ga_3O_{12}$ and $Y_3Ga_5O_{12}$ at ambient and high hydrostatic pressure, Phys. Chem. Chem. Phys. 18 (2016) 6683–6690.
[31] J. Ueda, P. Dorenbos, A.J.J. Bos, K. Kuroishi, S. Tanabe, Control of electron transfer between Ce^{3+} and Cr^{3+} in the $Y_3Al_{5-x}Ga_xO_{12}$ host via conduction band engineering, J. Mater. Chem. C 3 (2015) 5642–5651.
[32] K. Szczodrowski, J. Barzowska, N. Górecka, M. Grinberg, Stabilization of Eu^{3+} under a reductive atmosphere by the Al^{3+} co-doping of Sr_2SiO_4:Eu^{2+}/Eu^{3+}, RSC Adv. 6 (2016) 48001–48008.